JACS
JOURNAL OF THE AMERICAN CHEMICAL SOCIETY

Article

pubs.acs.org/JACS

# Hierarchical Assembly of Bioactive Amphiphilic Molecule Pairs into Supramolecular Nanofibril Self-Supportive Scaffolds for Stem Cell Differentiation

Zhe Wang,[†] Fuwu Zhang,[†] Zhantong Wang,[†] Yijing Liu,[†] Xiao Fu,[†,‡] Albert Jin,[‡] Bryant C. Yung,[†] Wei Chen,[†] Jing Fan,[†] Xiangyu Yang,[†] Gang Niu,[†] and Xiaoyuan Chen*[,†]

[†]Laboratory of Molecular Imaging and Nanomedicine and [‡]Laboratory of Cellular Imaging and Macromolecular Biophysics, National Institute of Biomedical Imaging and Bioengineering, National Institutes of Health, Bethesda, Maryland 20892, United States

Supporting Information

**ABSTRACT:** Molecular design of biomaterials with unique features recapitulating nature's niche to influence biological activities has been a prolific area of investigation in chemistry and material science. The extracellular matrix (ECM) provides a wealth of bioactive molecules in supporting cell proliferation, migration, and differentiation. The well-patterned fibril and intertwining architecture of the ECM profoundly influences cell behavior and development. Inspired by those features from the ECM, we attempted to integrate essential biological factors from the ECM to design bioactive molecules to construct artificial self-supportive ECM mimics to advance stem cell culture. The synthesized biomimic molecules are able to hierarchically self-assemble into nanofibril hydrogels in physiological buffer driven by cooperative effects of electrostatic interaction, van der Waals forces, and intermolecular hydrogen bonds. In addition, the hydrogel is designed to be degradable during cell culture, generating extra space to facilitate cell migration, expansion, and differentiation. We exploited the bioactive hydrogel as a growth-factor-free scaffold to support and accelerate neural stem cell adhesion, proliferation, and differentiation into functional neurons. Our study is a successful attempt to entirely use bioactive molecules for bottom-up self-assembly of new biomaterials mimicking the ECM to directly impact cell behaviors. Our strategy provides a new avenue in biomaterial design to advance tissue engineering and cell delivery.

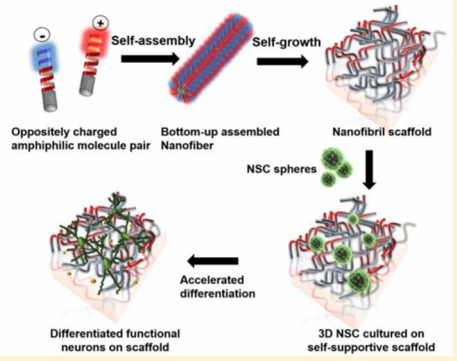


## INTRODUCTION

Molecular design of biomaterials with distinct merits as scaffolds to recapitulate the native extracellular matrices (ECM) niche in tissue regeneration and injury recovery has drawn increasing appreciation in medicine.[1,2] Interaction between cells and the ECM is a highly dynamic process.[3,4] The ECM provides synergistic biochemical and biophysical cues to direct cell proliferation, migration and differentiation,[5] whereas cells respond to the ECM stimuli to reshape their surrounding microenvironment.[6,7] Artificial scaffolds of synthetic polymers, such as polyethylene glycol (PEG)-based hydrogels,[5,8,9] or natural polymers, including collagen,[10] fibrin,[11] alginate,[12] and hyaluronic acid,[13,14] have been favorably explored to mimic the ECM to manipulate cell fate in vitro. The conventional approach of constructing an ECM mimic scaffold relies on extensive chemical modification and postprocessing steps using synthetic or natural polymers.[15] Recent advances in supramolecular self-assembly offer a simple and robust strategy for molecular design of scaffolds. Supramolecular self-assembly relies on amphiphilic building blocks which can assemble in the liquid phase, usually in aqueous solution, into well-defined three-dimensional (3D) hydrogels with diverse chemical compositions and biophysical features. The specially designed amphiphilic building blocks readily assemble into a wide variety of biophysical nanostructures such as nanofibers,[16−18] ribbons,[19,20] nanotubes,[21] or belts,[22] which provide fruitful options in scaffold topology to influence associated cell physiological conditions.[23] The design of amphiphilic molecules to self-assemble ECM mimics with defined mechanical strength and microstructure are highly instrumental for tissue engineering and drug/cell delivery.

Most artificial scaffolds recapitulate mechanical and topological properties of natural ECMs. These are, however, usually short of biochemical signal molecules critical to maintain regular cell proliferation and development. Additional modification of established scaffolds with adhesive and/or stimulating motifs are thus needed for successful 3D cell culture.[24,25] In several recent examples of hydrogel scaffold design, bioactive peptide epitopes derived from extracellular proteins were deliberately integrated into scaffolds to promote cellular adhesion, proliferation, and differentiation.[15,25−27] Stupp and co-workers reported an amphiphilic peptide molecule that incorporates a pentapeptide motif, Ile-Lys-Val-

**Received:** September 2, 2016
**Published:** October 24, 2016





DOI: 10.1021/jacs.6b09014
J. Am. Chem. Soc. 2016, 138, 15027−15034

Ala-Val (IKVAV), found in the laminin to self-assemble into a 3D nanofiber scaffold to induce stem cell differentiation.[26,28] A widely used peptide motif, Arg-Gly-Asp (RGD), derived from fibronectin, is able to promote cell adhesion and proliferation.[29] It has been successfully exploited in self-assembling hydrogels to support cell adhesion and migration in 3D cell culture systems.[30] Those seminal studies demonstrated the importance and feasibility of including bioactive peptide sequences in the designed scaffolds to impact cell behaviors. One particular challenge in such design, however, is the fact that cell proliferation and differentiation is a highly sophisticated process involving multiple ligand−receptor interactions. A single type of peptide epitope in the entire scaffold is limited in its ability to direct the complex biological behaviors of cells. The diverse molecular structures of self-assembling molecules provide us unprecedented opportunities. Integration of multiple bioactive components into the structure of individual building blocks of a scaffold is highly crucial to synergistically affect cell behavior and development. In addition, the various intermolecular interactions, such as hydrogen bonds, electrostatic interaction of oppositely charged molecules, hydrophobic−hydrophobic interaction, and $\pi-\pi$ stacking in $\beta$-sheet formation, provide a wide variety of assembly driving forces in molecular design. The design of molecules with temporal degradability is equally critical to sustainably release individual bioactive factors to interact with cells, as well as to generate extra space to accommodate cell growth, expansion and morphological changes, such as neurite outgrowth during neural stem cell (NSC) differentiation.[26,31,32]

In this study, we go beyond conventional single-component rigid bioactive scaffolds to develop a new molecular design strategy to build a self-supportive ECM mimetic scaffold (Scheme 1). Our study demonstrated two key traits in the design of bioactive scaffolds. The first trait is that the entire scaffold is composed of ECM-derived bioactive substances which cooperatively impart control of cellular activities. Most peptide motifs derived from ECM proteins may be positively or negatively charged in physiological fluids. The design of accompanying amino acid residues in molecular structure could alter the physicochemical characteristics of the target peptide sequences, while maintaining the bioactivities of those peptides. In addition, numerous small molecules from the ECM play key roles in regulating biochemical signals. The incorporation of small molecules in designed molecular structures is beneficial to influence cellular behavior, while defining the physicochemical features of such molecules. The second trait is that most previous studies have reported rigid scaffolds using native amide linkages in entire amphiphilic peptides.[33] Since amide bonds are nondegradable unless using specific enzymes, molecules thoroughly linked by amide bonds can hardly create a degradable and dynamic local environment to adapt to cell proliferation, expansion, and migration. In constructing a biodegradable molecule, researchers usually introduce dithiol bonds in the molecular structure to introduce cleavable sites in the original molecule. The dithiol bond is more likely cleaved intracellularly in the cytosol where high concentrations of glutathione produce a reducing environment. In the extracellular environment, however, dithiol bonds may not function well. In our study, we report a method of incorporating an ester bond to link the hydrophobic and hydrophilic domains by simple orthogonal conjugation chemistry. Many molecules, including small molecules and peptides, contain chemically accessible hydroxyl, carboxyl groups, or both in the chemical structure. This facilitates the conjugation of two desired molecules into a new one through the formation of a hydrolyzable ester bond. In turn, hydrolysis of the ester bond regains the native hydroxyl and carboxyl groups of the molecules and maintains their bioactivity. Based on these two molecular traits, the novel scaffold is based on hydrolyzable amphiphilic molecules overwhelmingly composed of multiple bioactive components. Primary NSCs cultured in this scaffold can proliferate and differentiate into functional neuronal subtypes in an accelerated manner. Our study presents a successful attempt to employ nature's motifs in conjunction with supramolecular self-assembly to design biomaterials to precisely manipulate cells.

**Scheme 1. Illustration of Oppositely Charged Amphiphilic Molecule Pairs for Bottom-Up Self-Assembly into a Self-Supportive Degradable Scaffold to Guide Neural Stem Cell Differentiation**

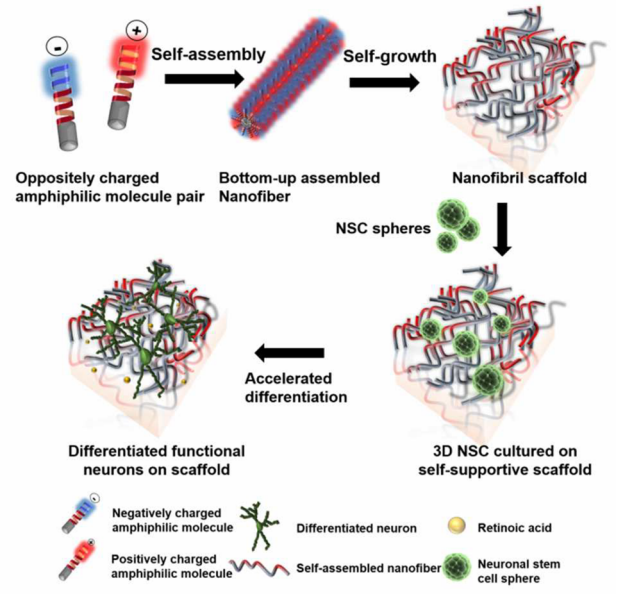


## EXPERIMENTAL DETAILS

**Synthesis and Characterization of Molecules.** *Materials.* All solvents used in this study were obtained from Sigma-Aldrich (St. Louis, MO). They were all obtained as HPLC-grade or higher and used directly without further purification. All Fmoc-protected amino acids, 2-(1H-benzotriazole-1-yl)-1,1,3,3-tetramethyluronium-hexafluorophosphate (HBTU), Rink Amide MBHA resin, and Wang resin were purchased from CS Bio. Co. (Menlo Park, CA). Retinoic acid, 2-cyano-6-hydroxylbenzylthiazole, 20% piperidine in dimethylformamide (DMF), and *N*,*N*-diisopropylethylamine (DIPEA) were received from Sigma-Aldrich (St. Louis, MO) and used as received without further purification.

*Synthesis of Self-Assembly Bioactive Molecules.* The standard Fmoc ([*N*-(9-fluorenyl)methoxycarbonyl]) solid-phase peptide synthesis (SPPS) was used to synthesize the oligopeptide fragment of each self-assembled molecule. Fmoc-D-cys(Trt)-OH was used at the N-terminus for the subsequent orthogonal conjugation with 2-cyano-6-hydroxylbenzylthiazole ((D-Cys)-GGGSEYIGSR-Wang; (D-Cys)-GGGSEPHSRN-Rink)). CS336X automated Peptide Synthesizer from CS Bio. Co. (Menlo Park, CA) was employed to synthesize the peptide at 0.1 mmol scale. During each reaction, Fmoc deprotection was carried out using 20% piperidine in DMF solution, which was programmed in the synthesizer. TFA/TIS/$H_2O$/EDT (93:2.5:2.5:2.5) cocktail was used for 2−3 h to cleave the peptide from


DOI: 10.1021/jacs.6b09014
J. Am. Chem. Soc. 2016, 138, 15027−15034

the respective resin. Rotatory evaporator was use to remove excess TFA, and the cleaved oligopeptide was precipitated in cold ether. Excess ether was used to wash the precipitate two times. The residual ether was removed by reduced pressure. The crude oligopeptide was separated using a $C_{18}$ semipreparative column on a Dionex Ultimate3000 HPLC system using gradient mobile phase: A: $H_2O$ (0.1% TFA); B: acetonitrile (0.1% TFA); 5% B/45−90% B/5% B over 40 min. Figure S1 shows the entire synthesis procedure.

The retinoic acid and 2-cyano-6-hydroxylbenzylthiazole ester was synthesized using the following protocol. In brief, 300 mg of all *trans* retinoic acid (1 mmol) was mixed with 1.1 equiv (210 mg) of 2-cyano-6-hydroxylbenzylthiazole in 18 mL of methylene chloride (DCM) and 2 mL of acetonitrile (ACN) cosolvent at room temperature. In the above cosolvent, the following chemicals were added to initiate the ester conjugation: 1 g of *N*,*N*′-dicyclohexylcarbodiimide (DCC) (5 mmol) and 61 mg of 4-(dimethylamino)pyridine (DMAP) (0.5 mmol). The entire mixture was dispensed into a 100 mL round-bottomed flask with a magnetic stirring bar. The reaction was carried out overnight at room temperature. The cosolvent was evaporated by rotatory evaporator to yield a yellow powder. The product was purified by flash chromatography (Teledyne ISCO CombiFlash) using a prepacked silica column using gradient ethyl ecetate and hexane cosolvent as the mobile phase: 98% hexane/2% ethyl estate to 90% hexane/15% ethyl acetate over 20 min. The resultant ester product (RA ester) was readily separated from the raw materials as the final product is less polar than any of the raw materials. Figure S2 shows the entire synthesis procedure.

To conjugate RA ester with oligopeptide by the ring-forming reaction of thiol and amine groups on N-terminal D-cysteine with the cyanide group of 2-cyano-6-hydroxylbenzylthiazole, the following reaction procedure was conducted: A 1.2:1 molar ratio of RA ester with oligopeptide was dissolved in 2 mL of DMF with moderate shaking at room temperature for 30 min. The resulting product was precipitated from cold ether (10 mL), and the yellow precipitate was washed additionally two times with cold ether. Molecule **1** precipitate formed a slurry solid, while molecule **2** yielded a crystal form. The precipitate was further purified by semipreparative HPLC following the procedure as described above.

*Self-Assembled Bioactive Hydrogel Preparation.* To form a self-assembled hydrogel, molecules **1** and **2** were separately dissolved in PBS buffer at 1% (w/v) scale. The solution containing molecule **1** (solution 1) was adjusted to pH ∼8 using 0.1 N NaOH to ensure complete dissolution, whereas solution having molecule **2** (solution 2) was adjusted to pH ∼6 using 0.1 N HCl to facilitate solubility. pH paper was used in the entire procedure to ensure pH value accuracy and consistency. To self-assemble the bioactive hydrogel, solutions of **1** and **2** at equal volumes were mixed and vigorously vortexed. White aggregate was observed immediately after mixing, whereas the mixing solution became transparent after vortexing a few minutes. The solution was kept undisturbed for 30 min during which the molecules self-assembled into a hydrogel.

Upon mixing two oppositely charged peptides, the sudden pH change in the solution resulted in the formation of white aggregates. The aggregates dispersed in the final neutral solution in which two individually oppositely charged molecules interacted by electrostatic interaction to self-assemble into supramolecular structures along with the van der Waals force arising from hydrophobic interaction between retinoic acids. In addition, the planar structure of RA is likely to form intramolecular $\pi-\pi$ stacking, which facilitated the $\beta$-sheet super-structure formation in the final product.

**Isolation and Culture of Primary Neural Stem Cells.** *Materials.* Primary NSC culture medium, DMEM, and Ham's F-12 medium in a 1:1 ratio (DMEM/F12), Neurobasal medium, B27 serum-free supplement, N2 supplement, GlutaMAX were all obtained from Invitrogen. Laminin and poly-D-lysine were obtained from Roche Life Science (Indianapolis, IN). Basic fibroblast growth factor (bFGF) and epidermal growth factor (EGF) were purchased from PeproTech (Rocky Hill, NJ). To 500 mL of DMEM/F-12 medium was added 5 mL of $N_2$ and 5 mL of L-glutamine. Before passaging NSCs, additional bFGF (20 ng/mL) and EGF (100 ng/mL) were added to the solution. To prepare a NSC differentiation medium, neurobasal medium was modified with B27 serum-free supplement and GlutaMAX I supplement. No antibiotics were added in the entire experiment. The brain dissection enzyme mix was prepared as follows: 10 mg of type I−S hyaluronidase (Sigma-Aldrich) was mixed with 10 mL of 0.25% Trypsin solution. The mixture was aliquoted and kept frozen until use.

*Isolation and Culture of NSCs.* We strictly followed the principles and procedures outlined in the NIH guide for the care and use of laboratory animals which were preapproved by the Institutional Animal Care and Use Committee of the NIH clinical center. Transgenic FVB mice (Jackson Lab, Bar Harbor, ME) were used as the neonatal mouse donor. The NSC isolation and culture procedures were adopted from literature with modification in our laboratory.[34,35] Briefly, 1 day old neonatal mice were euthanized and immediately sterilized to isolate the brain tissue from which the forefront brain tissue was isolated and dispersed in NSC culture medium. Removal of the skull using forceps and stripping off the remaining meninges from the brain tissue was accomplished using forceps. Since we have no special requirement for specific region of neurons, we used the whole neonatal brain to generate neurospheres (a collection of 1 day old neonatal pups, $n$ = 3−5 ). The brain was cut into 4 pieces using a sterilized scalpel. The brain pieces were digested in the digestion enzyme mixture for 30 min at 37 °C. The digested tissue was centrifuged at 1000 rpm for 3 min, and the settled neurosphere pellets were then harvested and dispersed in NSC culture medium. A sterile Pasteur pipet was used to gently blow the NSC suspension to generate small pieces of neurospheres for subsequent culturing. The NSC spheres are a nonadherent culture. The medium was changed every other day. In the first 3−5 days, the culture was a mixture of NSCs with other blood cells and immune cells, whereas NSC spheres became the predominant cells after 1 week of culturing and medium change. The medium with supplements and growth factors in it facilitates the NSC sphere selection process.

*Differentiation of NSCs in 2D and 3D Culture Systems.* The cultured NSCs were used for differentiation study at passage 3−4. For PDL and Laminin/PDL coating 2D culture, the culture substrates were precoated with PDL or Laminin/PDL 24 h before NSC seeding for differentiation. For the self-assembled (SA) bioactive hydrogel 3D culture, the hydrogel was prepared as stated above and transferred to the cell culture substrate as a solid gel; the NSC spheres suspended in the differentiation medium were mixed with the SA gel gently. The NSC mixed gel was incubated in the incubator untouched for 30 min; then, 200 $\mu$L of differentiation medium was added on top of the solid gel. In general, 5000−8000 cells were cultured on the 12 mm glass coverslip insert used as the substrate in each well of a 24-well plate. The 2D culture system used regular neuronal culture medium composed of Neurobasal medium supplemented with B27 serum-free supplement, GlutaMAX I supplement, and 1 $\mu$M retinoic acid solution (stock solution prepared in DMSO at 1 mM concentration). For the SA bioactive hydrogel culture, DMEM/F12 mixed medium with bFGF (20 ng/mL) was used without any supplemented growth factors or differentiating reagents.

*Cell Viability and Live/Dead Staining.* The cell viability assay was conducted using LIVE/DEAD Viability/Cytotoxicity Kit (Molecular Probes) according to the manufacturer's protocol. Briefly, 10 $\mu$L of 2 mM ethidium homodimer-1 (EthD-1) stock solution was added into 5 mL of PBS to yield the 4 $\mu$M EthD-1 working solution. Then, 2 $\mu$L of calcium AM stock solution (4 mM) was added into 5 mL of EthD-1 working solution. Vortexing of the mixture solution was completed to ensure homogeneity. The resulting final working solution contained 1.5 $\mu$M calcium AM and 4 $\mu$M EthD-1. Aspiration of the culture medium from both 2D and 3D cultures, followed by gentle rinse of the cultured cells using warm PBS, was performed once. After aspirating the rinsing PBS, the prepared staining solution was added into each culture well at a 250 $\mu$L volume. The culture was transferred to an incubator for 20 min. Upon completion of incubation, the staining solution was removed, and cells were rinsed once with PBS. The fluorescent signals from calcium AM and EthD-1 were read by Olympus ×82 fluorescence microscopy using GFP and RFP channels.


DOI: 10.1021/jacs.6b09014
J. Am. Chem. Soc. 2016, 138, 15027−15034

Live cell ratio was calculated as the following: Live cell ratio = green fluorescence positive cell number/(green fluorescence positive cell number + red fluorescence positive cell number) × 100%.

*Immunocytochemistry Staining.* Cell culture medium was aspirated, and cells were gently rinsed with prewarmed PBS once. Z-fix Formalin (Anatech) was applied to each cell culture to fix cells for 10 min. After getting rid of the fixing solution, cells were rinsed two times using PBS; 0.1% Triton X-100 in PBS was added to each cell culture to permeabilize the cell membrane for 5 min. After aspirating the Triton X-100 solution, the cells were rinsed twice using PBS. This was followed by incubation of cells with 1% BSA (bovine serum albumin) PBS solution for immunoblocking for 30 min. The blocking solution was aspirated, and primary antibodies against βIII tubulin or synapsin I (Cell Signaling Inc.) were diluted in a 1:300 ratio in 1% BSA PBS solution and applied to cells to incubate for 4 h at room temperature. Alternatively, this primary antibody procedure could be done overnight at 4 °C in a cold room. After incubating with primary antibodies, cells were rinsed with 0.05% Tween 20/PBS solution 5 times, followed by incubation with fluorophore-labeled secondary antibodies against the host isotypes at 1:500 dilution in 1% BSA PBS solution for 1 h at room temperature. For F-actin costaining with synapsin I, Alexa Fluor 488 phalloidin (Molecular Probes) solution was mixed with the secondary antibody solution for coincubation. Then, the secondary antibody solution was aspirated, and cells were rinsed 5 times using 0.05% Tween 20. The cell nucleus was counterstained by DAPI in the mounting medium (Vector Laboratories, Burlingame, CA). Cell images were captured using Olympus ×82 fluorescence microscopy or Olympus FV10i confocal microscopy.

*Neurite Outgrowth Counting.* We used a reported method to estimate the neurite length with slight modification.[36] In general, each image was evenly divided by 12 lines vertically and horizontally to yield 13 × 13 = 169 cubes. Positive neurite staining from each neuronal cluster in each cube was manually measured, and the total length of neurite was calculated by adding the whole measured length. Four to five individual pictures obtained from different regions or slides were calculated for statistical analysis.

*Electrophysiology Recording.* Differentiated cell firing action potential was recorded by current clamp whole-cell configuration.[37,38] Cells were preselected based on the morphology, and previous βIII tubulin staining results suggested the generation of mature neurons in the differentiated culture system. The pipet solution (composed of, in mM, 124 NaCl, 3 KCl, 26 $NaHCO_3$, 1.25 $NaH_2PO_4$, 2.5 $CaCl_2$, 1.3 $MgSO_4$ and 10 D-glucose) was maintained during the current clamp experiment. Step current was injected to induce firing potential. Whole-cell current was recorded, and stimuli were delivered at 10 mV increments.

## RESULTS AND DISCUSSION

**Molecular Design.** In our design, two peptide epitopes derived from ECM proteins responsible for cell adhesion and proliferation, and a small molecule morphogen directing stem cell differentiation are incorporated in the scaffold structure. The three components each having distinctive physiochemical features constitute the main bodies of two oppositely charged amphiphilic molecules (Scheme 1 and Figure 1A). There is a growing body of evidence that combination of two or more biological signals in ECM in an intimate manner produce synergistic effects in cell responses.[39,40]

Among various ECM proteins, laminin, a major component of basal lamina, plays a key role in regulating cell adhesion, migration, and differentiation.[41] One pentapeptide sequence, YIGSR, derived from laminin, promotes cell adhesion and differentiation by binding to 67LR (67 kDa laminin receptor).[42] Another pentapeptide, PHSRN, derived from fibronectin, supports the attachment of cells to their surroundings.[43] In our approach, we designed two oppositely charged peptide

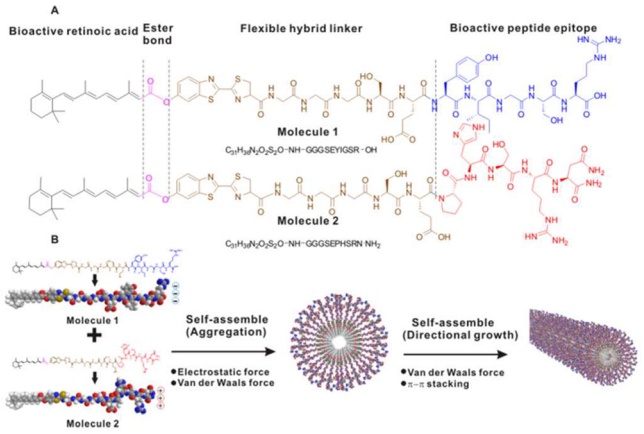


**Figure 1.** (A) Chemical structures of amphiphilic bioactive molecule pairs used for self-assembly. (B) Schematic illustration of hierarchical self-assembly of two oppositely charged amphiphilic molecule pairs into the interim micellar structure and eventually the fibril structure.

sequences, each incorporating one oligopeptide in the structure. For peptide sequence containing YIGSR (molecule **1**), we inserted a negatively charged Asp (D) residue following the YIGSR sequence and kept the C-terminal end in the carboxylic form. This renders the entire sequence negatively charged. In molecule **2**, the bioactive pentapeptide sequence is PHSRN followed by the identical oligopeptide sequence used in molecule **1**, while the C-terminus was modified with an amide, leaving the entirty of molecule **2** positively charged. The third component provides hydrophobic driving force for self-assembly and simultaneously directs NSC differentiation as a potent biological morphogen.[44] All-trans retinoic acid (RA) meets all the requisites and is thus chosen as the hydrophobic fragment in the molecular design.[45] To gradually liberate RA from the solid scaffold, an ester bond is introduced by conjugating RA with the hydroxyl group of 2-cyano-6-hydroxylbenzylthiazole (Figure S1), which further reacts with N-terminal cysteine (C) residue of the above peptide sequences to form a 5-membered heterocyclic structure (Figure S2). This creates a hydrolyzable ester center in each amphiphilic molecule structure (Figure 1). The GGGS sequence in the structure serves as a flexible linker and provides spatial separation between hydrophobic and hydrophilic fragments facilitating self-assembly.[46]

Molecule **1** at the concentration of 1 mg/mL is readily soluble at neutral pH but precipitates when the pH is lower than 5.5. Molecule **2** at the same concentration (1 mg/mL) is soluble between pH 6.5 and 8. The imidazole side chain ($pK_a$ 6.0) of the His residue in molecule **2** potentially serves as a buffering group to tolerate pH variations.[47,48] Upon mixing of the oppositely charged molecules **1** and **2** (1 mg/mL) at neutral pH, an opaque precipitate formed within seconds. When each molecule concentration was increased to 1% (w/v), the mixing of two solutions at neutral pH yielded a solid hydrogel within 30 min (Figures 2 and S4). In contrast, a single component of either molecule **1** or **2** alone could not readily assemble into a molecularly packed prolonged nanofibril structure to yield a firm hydrogel (Figure S5).

Our molecular design strategy provides an interesting way of supramolecular self-assembly. This concept can be applied to other peptide sequences mimicking ECM proteins to self-assemble into fibrils, albeit slight morphological changes (Figure S6). The hydrophobic small molecule portion could


DOI: 10.1021/jacs.6b09014
J. Am. Chem. Soc. 2016, 138, 15027−15034

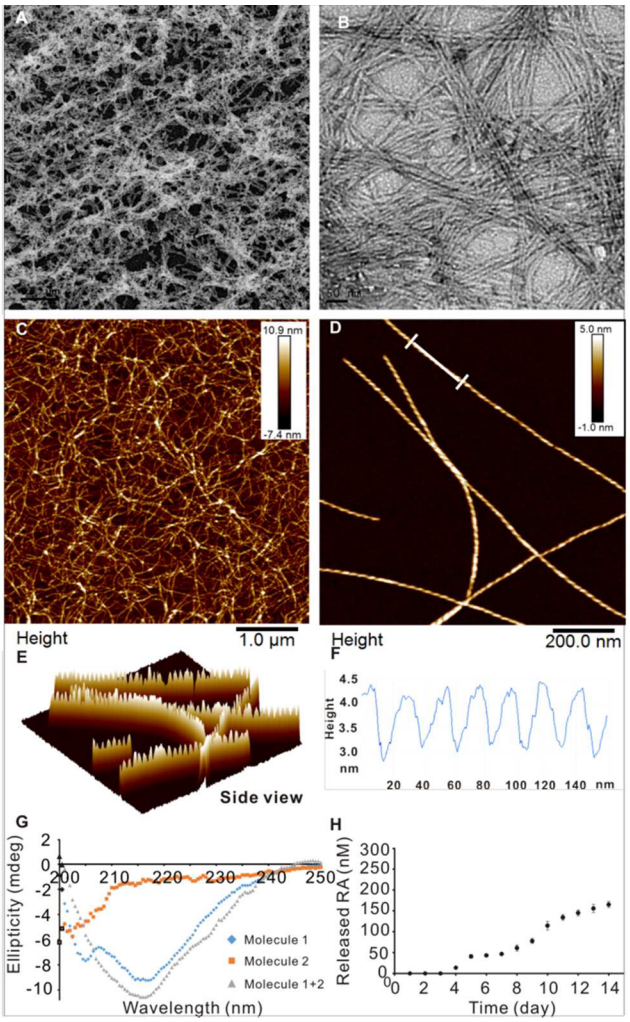


**Figure 2.** (A) Low-magnification and (B) high-magnification TEM images of self-assembled nanofibers. (C) Low-magnification and (D) high-magnification AFM images of self-assembled nanofibers. (E) Side view of nanofibers from image D. Nanofiber height analysis in the AFM image D. The height analysis profile is indicating the white line selected area in D. (G) CD analysis of self-assembly of nanofiber in different molecule compositions. (H) Retinoic acid release profile from assembled hydrogel.

be replaced by hydrophobic oligopeptide sequences with defined biological functions.

**Self-Assembly of Nanofibrous Scaffolds and Characterization.** Supramolecular self-assembly of two peptide mixtures under physiological condition transform the liquid phase into a solid hydrogel combining two peptide motifs into a single fibril (Figure 2). The electrostatic interactions of hydrophilic oligopeptides, hydrophobic aggregation of RA molecules, and strong intramolecular hydrogen bonds synergistically provide the driving forces to trigger the hierarchical self-assembly process. Similar to the reported single peptide motif system,[26] the assembled nanofibers composed of two bioactive peptides derived from different ECM proteins display the charged hydrophilic bioactive epitopes on the surface of fibril structures. Meanwhile, the hydrophobic molecule, RA, is sequestered in the center. The formation kinetics of the fibril structure reported earlier by Tirrell and co-workers was to undergo two dynamic stages where spherical micelles were first formed as a transient morphology followed by filamentous growth of nanofibers after prolonged incubation time.[49] The transmission electron microscopy (TEM) image shows nanofibers after the coassembly process at 1% peptide concentration (Figure 2A,B). Low-magnification TEM (Figure 2A) shows the porous feature of the formed nanofiber hydrogel. This feature is optimal to trap most types of cells including NSC clusters, while permeating nutrients and inorganic salts in the medium to support cell proliferation and differentiation.[50] Atomic force microscope (AFM) (Figure 2C–F) reveals that individual nanofiber is stacked in a spirally twisted pattern, and the average height of each nanofiber is about 4 nm (Figure 2F). Both TEM and AFM images present homogeneous nanoscale fibrils intertwined to form a 3D network. As an ECM mimetic, the topological pattern arisen from nanofibers in the hydrogel scaffold has salient roles in directing NSC behavior.[51] At a concentration of 0.4 mM, the circular dichroism (CD) spectrum of **1** reveals that this molecule is composed of combined random coil and $\beta$-sheet (216 nm) characters (Figure 2G), and the CD spectrum of molecule **2** shows a predominantly random coil pattern. This could be attributed to partial (molecule **1**) and complete (molecule **2**) intramolecular electrostatic repulsion in charged molecules. Upon mixing equal molar amounts of molecules **1** and **2**, the CD spectrum exhibits a typical $\beta$-sheet signature with intense signal at 216 nm (Figure 2G). The electronic structure reflected by the CD spectrum corroborates with what was observed from microscope images. In our system, nanofibers are mostly formed instead of other nanostructures, such as belts, ribbons, or tapes, which share similar $\beta$-sheet assembling mechanism but are driven by distinctively different molecular driving forces.[52] This difference is mainly attributed to the short gelation time (usually less than 30 min) and combined effects of the intramolecular electronic repulsion and intermolecular attraction during the peptide self-assembly process. Recent advances in the understanding of peptide assembly have identified the essence of electrostatic interactions in determining the degree of molecule intertwining and peptide morphology.[53,54] Our results are consistent with other reports on self-assembly mechanisms. Next, we evaluated the RA release profile of the formed hydrogel in buffer within a fixed time period (14 days). The preformed hydrogel was put in PBS buffer at 1:2 volume ratio and incubated at 37 °C. HPLC analysis indicates that RA has a two-stage release profile: In the first 3 days, a trace amount of RA molecule was detected, whereas starting from day 4, an accelerated amount of RA molecule was present in solution (Figure 2H). It was reported that locally concentrated RA molecules can stimulate neural progenitor cell differentiation into neurons more effectively than can freely dispersed RA in solution.[55] We calculated the released RA concentration in our system, which is 38.0 ± 2.3 nM on day 5 and 157.1 ± 5.6 nM on day 10. The intimate contact between released RA and loaded cells in the hydrogel could promote cell differentiation.

**Self-Assembled Scaffold to Direct Neural Stem Cell Differentiation.** Our goal of constructing such a bioactive hydrogel system is to use it as a self-supporting scaffold to direct neural stem cell differention with minimal supplementing nutrients or growth factors. To avoid the disadvantage of 2D cell culture in traditional Petri dishes, extensive efforts have been made to fabricate various engineered 3D scaffolds to mimic the natural cell/tissue developmental milieu.[2,20,56] Our molecular design advanced the current design protocol to simultaneously incorporate three important ECM-derived factors which self-assembled into a fibrous gel to synergistically


DOI: 10.1021/jacs.6b09014
J. Am. Chem. Soc. 2016, 138, 15027–15034

promote NSC growth, neurite outgrowth and differentiation into neurons. We cultured primary neural stem/progenitor cells (passage 3) on the bioactive scaffold prepared in cell culture medium at 1:1 volume ratio. We also employed poly-D-lysine (PDL) and laminin/PDL (Lam/PDL) coated substrates as conventional culture controls. One day after culturing, we observed remarkably different neurosphere morphology change (Figure 3A). The outgrowth of branched neurite was

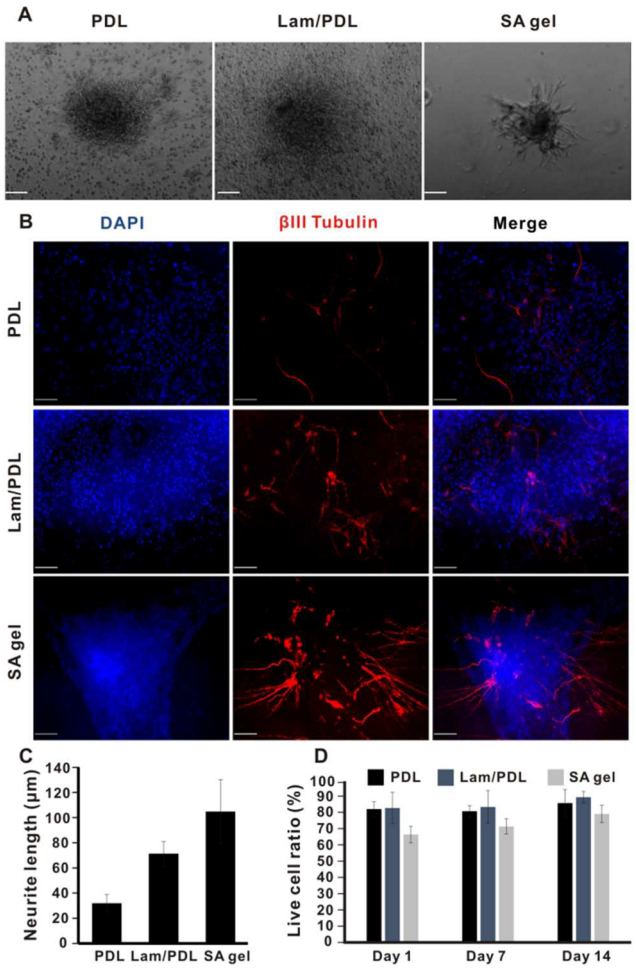


**Figure 3.** (A) Images of neural stem cell sphere attachment in different culture environment. Scale = 50 nm. (B) Neurite outgrowth staining ($\beta$III tubulin) of differentiating NSCs. Scale = 50 nm. (C) Neurite length counting from $\beta$III tubulin staining images. $n$ = 4–5. (D) Live/Dead cell staining of differentiating NSCs at different times. $n$ = 3.

prominent in the bioactive gel, where as neurospheres grew on PDL and laminin/PDL substrates were not able to fully develop well branched neurite outgrowth at such an early time point. After culturing cells on the respective substrate for 5 days, we used antibody against $\beta$III tubulin, a neuron specific biomarker[57] to stain the neurospheres. We observed a strong $\beta$III tubulin network development in the bioactive hydrogel culture which exceeded the effects of laminin/PDL coating on NSC development (Figure 3B).[58] Statistical analysis of $\beta$III tubulin length by counting 3 images of different nanospheres showed significant differences between the three culture groups (Figure 3B and C). In addition, all the culture groups demonstrated healthy cellular ultrastructure without noticeable detrimental effects to cells as indicated by live/dead cell staining (Figure 3D).

To assess the neuron-specific function of differentiated NSCs, we used immunocytochemistry to establish the in vitro differentiation consequences in three culture systems. The synapse is a structure in neuronal communication in which a neuron transmits electrical or chemical signal to another neuron or other cells in the vicinity.[59] To identify the establishment of synapse in the differentiating neural stem cells in the bioactive scaffold, we selected synapsin I, a protein presented at the terminal of axon and highly involved in synapse,[60] as a biomarker in staining cultured cells. Figure 4A

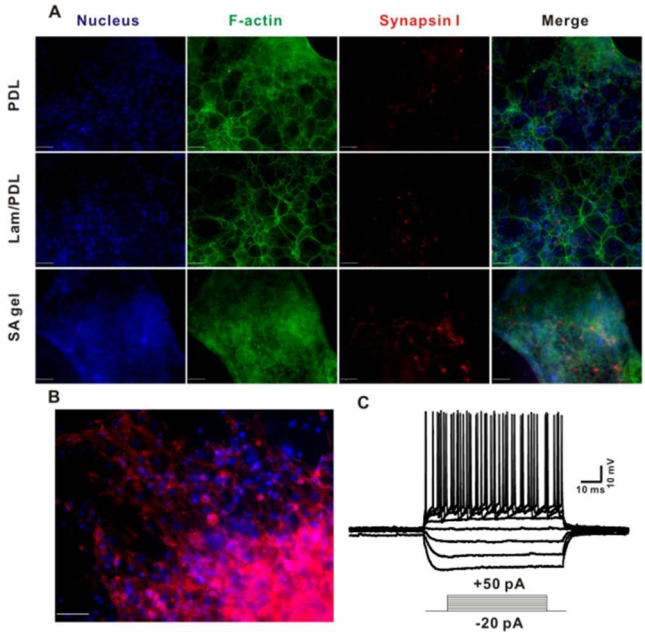


**Figure 4.** (A) Synaptic protein, synapsin I, staining of differentiated NSCs at day 7. Scale = 50 $\mu$m. (B) $\beta$III tubulin staining of differentiated NSCs at day 14. Scale = 50 $\mu$m. (C) Electrophysiological recording of action potential firing from selected NSC differentiated neurons from the self-assembly bioactive hydrogel.

showed extensive presence of synapsin I in the bioactive hydrogel system after 5 days of culturing. In contrast, laminin/PDL group had dramatically decreased level, and PDL group showed marginal level of synapsin I staining. It appears that 5 days of culturing in the bioactive hydrogel facilitated direction of NSC differentiation into neurons with proper neuronal activities. To further validate that the bioactive hydrogel is able to generate an array of functional neurons, we cultured cells in the scaffold for 14 days before we conducted electrophysiological study on selected cells. Extensive neurite outgrowth was established on day 14 by $\beta$III tubulin staining (Figure 4B). After applying increasing current injection from −20 to +50 pA to depolarize a selected cell, the current clamp recorded action potential firing (Figure 4C), indicative of mature and functional neuron in culture.[61] We, however, did not find any positive neuron firing output in the other two culture systems. This finding confirms that the designed bioactive hydrogel is self-supportive and able to direct the neural stem/progenitor cell differentiation into mature neuron within a short period of time, overcoming limitations of two commonly used 2D culture system coatings, PDL and laminin/PDL.


DOI: 10.1021/jacs.6b09014
J. Am. Chem. Soc. 2016, 138, 15027–15034

## CONCLUSIONS

In this report, we successfully demonstrated a new molecular design strategy to develop a degradable bioactive scaffold entirely composed of multiple ECM-derived elements and explored the use of this scaffold to efficiently guide NSC differentiation into functional neurons. This scaffold bears enormous potential for in vitro 3D cell manipulation and can be incorporated with microinjection technologies for stem cell transplants in neuronal tissue engineering and cell delivery for central nervous system (CNS) disease therapy or traumatic brain injury (TBI) recovery.

## ASSOCIATED CONTENT

### Supporting Information

The Supporting Information is available free of charge on the ACS Publications website at DOI: 10.1021/jacs.6b09014.

Molecule synthesis, characterization, and other relevant materials (PDF)

## AUTHOR INFORMATION


### Corresponding Author

*E-mail: Shawn.Chen@nih.gov.


### Notes

The authors declare no competing financial interest.

## ACKNOWLEDGMENTS

This study was supported, in part, by the Center for Neuroscience and Regenerative Medicine (CNRM) program grant from the Department of Defense (DoD) and the Intramural Research Program (IRP) of National Institutes of Health (NIH).

## REFERENCES


(1) Lee, K. Y.; Mooney, D. J. *Chem. Rev.* **2001**, *101*, 1869.
(2) Zhang, S. *Nat. Biotechnol.* **2003**, *21*, 1171.
(3) Epstein, I. R.; Xu, B. *Nat. Nanotechnol.* **2016**, *11*, 312.
(4) Yokoi, H.; Kinoshita, T.; Zhang, S. *Proc. Natl. Acad. Sci. U. S. A.* **2005**, *102*, 8414.
(5) Caiazzo, M.; Okawa, Y.; Ranga, A.; Piersigilli, A.; Tabata, Y.; Lutolf, M. P. *Nat. Mater.* **2016**, *15*, 344.
(6) Kharkar, P. M.; Kiick, K. L.; Kloxin, A. M. *Chem. Soc. Rev.* **2013**, *42*, 7335.
(7) Cushing, M. C.; Anseth, K. S. *Science* **2007**, *316*, 1133.
(8) Higginson, C. J.; Kim, S. Y.; Peláez-Fernández, M.; Fernandez-Nieves, A.; Finn, M. G. *J. Am. Chem. Soc.* **2015**, *137*, 4984.
(9) Kloxin, A. M.; Kasko, A. M.; Salinas, C. N.; Anseth, K. S. *Science* **2009**, *324*, 59.
(10) Oh, H. H.; Ko, Y. G.; Lu, H.; Kawazoe, N.; Chen, G. *Adv. Mater.* **2012**, *24*, 4311.
(11) Ye, Q.; Zund, G.; Benedikt, P.; Jockenhoevel, S.; Hoerstrup, S. P.; Sakyama, S.; Hubbell, J. A.; Turina, M. *Eur. J. Cardiothorac. Surg.* **2000**, *17*, 587.
(12) Wang, C. C.; Yang, K. C.; Lin, K. H.; Liu, H. C.; Lin, F. H. *Biomaterials* **2011**, *32*, 7118.
(13) Collins, M. N.; Birkinshaw, C. *Carbohydr. Polym.* **2013**, *92*, 1262.
(14) Gerecht, S.; Burdick, J. A.; Ferreira, L. S.; Townsend, S. A.; Langer, R.; Vunjak-Novakovic, G. *Proc. Natl. Acad. Sci. U. S. A.* **2007**, *104*, 11298.
(15) Du, X.; Zhou, J.; Shi, J.; Xu, B. *Chem. Rev.* **2015**, *115*, 13165.
(16) Diegelmann, S. R.; Hartman, N.; Markovic, N.; Tovar, J. D. J. *J. Am. Chem. Soc.* **2012**, *134*, 2028.
(17) Cui, H.; Webber, M. J.; Stupp, S. I. *Biopolymers* **2010**, *94*, 1.
(18) Lamm, M. S.; Rajagopal, K.; Schneider, J. P.; Pochan, D. J. *J. Am. Chem. Soc.* **2005**, *127*, 16692.
(19) Pashuck, E. T.; Stupp, S. I. *J. Am. Chem. Soc.* **2010**, *132*, 8819.
(20) Zhang, S.; Andreasen, M.; Nielsen, J. T.; Liu, L.; Nielsen, E. H.; Song, J.; Ji, G.; Sun, F.; Skrydstrup, T.; Besenbacher, F.; Nielsen, N. C.; Otzen, D. E.; Dong, M. *Proc. Natl. Acad. Sci. U. S. A.* **2013**, *110*, 2798.
(21) Ziserman, L.; Lee, H. Y.; Raghavan, S. R.; Mor, A.; Danino, D. J. *J. Am. Chem. Soc.* **2011**, *133*, 2511.
(22) Cui, H.; Cheetham, A. G.; Pashuck, E. T.; Stupp, S. I. *J. Am. Chem. Soc.* **2014**, *136*, 12461.
(23) Berthiaume, F.; Moghe, P. V.; Toner, M.; Yarmush, M. L. *FASEB J.* **1996**, *10*, 1471.
(24) Webber, M. J.; Appel, E. A.; Meijer, E. W.; Langer, R. *Nat. Mater.* **2015**, *15*, 13.
(25) Holmes, T. C.; de Lacalle, S.; Su, X.; Liu, G.; Rich, A.; Zhang, S. *Proc. Natl. Acad. Sci. U. S. A.* **2000**, *97*, 6728.
(26) Silva, G. A.; Czeisler, C.; Niece, K. L.; Beniash, E.; Harrington, D. A.; Kessler, J. A.; Stupp, S. I. *Science* **2004**, *303*, 1352.
(27) Chiu, L. L.; Radisic, M.; Vunjak-Novakovic, G. *Macromol. Biosci.* **2010**, *10*, 1286.
(28) Tysseling, V. M.; Sahni, V.; Pashuck, E. T.; Birch, D.; Hebert, A.; Czeisler, C.; Stupp, S. I.; Kessler, J. A. J. *J. Neurosci. Res.* **2010**, *88*, 3161.
(29) Xiong, J. P.; Stehle, T.; Zhang, R.; Joachimiak, A.; Frech, M.; Goodman, S. L.; Arnaout, M. A. *Science* **2002**, *296*, 151.
(30) Kisiday, J.; Jin, M.; Kurz, B.; Hung, H.; Semino, C.; Zhang, S.; Grodzinsky, A. J. *Proc. Natl. Acad. Sci. U. S. A.* **2002**, *99*, 9996.
(31) Gu, Q. H.; Yu, D.; Hu, Z.; Liu, X.; Yang, Y.; Luo, Y.; Zhu, J.; Li, Z. *Nat. Commun.* **2015**, *6*, 6789.
(32) Liu, X.; Gu, Q. H.; Duan, K.; Li, Z. J. *J. Neurosci.* **2014**, *34*, 8741.
(33) Niece, K. L.; Hartgerink, J. D.; Donners, J. J.; Stupp, S. I. *J. Am. Chem. Soc.* **2003**, *125*, 7146.
(34) Giachino, C.; Basak, O.; Taylor, V. *Methods Mol. Biol.* **2009**, *482*, 143.
(35) Guo, W.; Patzlaff, N. E.; Jobe, E. M.; Zhao, X. *Nat. Protoc.* **2012**, *7*, 2005.
(36) Ronn, L. C.; Ralets, I.; Hartz, B. P.; Bech, M.; Berezin, A.; Berezin, V.; Møller, A.; Bock, E. J. *J. Neurosci. Methods* **2000**, *100*, 25.
(37) Vierbuchen, T.; Ostermeier, A.; Pang, Z. P.; Kokubu, Y.; Sudhof, T. C.; Wernig, M. *Nature* **2010**, *463*, 1035.
(38) Zhao, W. D.; Hamid, E.; Shin, W.; Wen, P. J.; Krystofiak, E. S.; Villarreal, S. A.; Chiang, H. C.; Kachar, B.; Wu, L. G. *Nature* **2016**, *534*, 548.
(39) Tong, Y. W.; Shoichet, M. S. *Biomaterials* **2001**, *22*, 1029.
(40) Hynes, R. O.; Lander, A. D. *Cell* **1992**, *68*, 303.
(41) Timpl, R.; Rohde, H.; Robey, P. G.; Rennard, S. I.; Foidart, J. M.; Martin, G. R. *J. Biol. Chem.* **1979**, *254*, 9933.
(42) Cooke, M. J.; Zahir, T.; Phillips, S. R.; Shah, D. S.; Athey, D.; Lakey, J. H.; Shoichet, M. S.; Przyborski, S. A. *J. Biomed. Mater. Res., Part A* **2009**, *93*, 824.
(43) Feng, Y.; Mrksich, M. *Biochemistry* **2004**, *43*, 15811.
(44) Jacobs, S.; Lie, D. C.; DeCicco, K. L.; Shi, Y.; DeLuca, L. M.; Gage, F. H.; Evans, R. M. *Proc. Natl. Acad. Sci. U. S. A.* **2006**, *103*, 3902.
(45) Wang, Z.; Zhang, R.; Wang, Z.; Wang, H. F.; Wang, Y.; Zhao, J.; Wang, F.; Li, W.; Niu, G.; Kiesewetter, D. O.; Chen, X. *ACS Nano* **2014**, *8*, 12386.
(46) Thota, B. N.; Urner, L. H.; Haag, R. *Chem. Rev.* **2016**, *116*, 2079.
(47) Hansen, A. L.; Kay, L. E. *Proc. Natl. Acad. Sci. U. S. A.* **2014**, *111*, E1705.
(48) Li, S.; Hong, M. J. *J. Am. Chem. Soc.* **2011**, *133*, 1534.
(49) Shimada, T.; Sakamoto, N.; Motokawa, R.; Koizumi, S.; Tirrell, M. J. *J. Phys. Chem. B* **2012**, *116*, 240.
(50) Kim, J.; Li, W. A.; Choi, Y.; Lewin, S. A.; Verbeke, C. S.; Dranoff, G.; Mooney, D. J. *Nat. Biotechnol.* **2014**, *33*, 64.
(51) Qi, L.; Li, N.; Huang, R.; Song, Q.; Wang, L.; Zhang, Q.; Su, R.; Kong, T.; Tang, M.; Cheng, G. *PLoS One* **2013**, *8*, e59022.
(52) Hu, Y.; Lin, R.; Zhang, P.; Fern, J.; Cheetham, A. G.; Patel, K.; Schulman, R.; Kan, C.; Cui, H. *ACS Nano* **2016**, *10*, 880.




DOI: 10.1021/jacs.6b09014
*J. Am. Chem. Soc.* 2016, 138, 15027−15034

(53) Ruggeri, F. S.; Adamcik, J.; Jeong, J. S.; Lashuel, H. A.; Mezzenga, R.; Dietler, G. *Angew. Chem., Int. Ed.* **2015**, *54*, 2462.
(54) Usov, I.; Mezzenga, R. *ACS Nano* **2014**, *8*, 11035.
(55) Santos, T.; Ferreira, R.; Maia, J.; Agasse, F.; Xapelli, S.; Cortes, L.; Braganca, J.; Malva, J. O.; Ferreira, L.; Bernardino, L. *ACS Nano* **2012**, *6*, 10463.
(56) Higuchi, A.; Ling, Q. D.; Hsu, S. T.; Umezawa, A. *Chem. Rev.* **2012**, *112*, 4507.
(57) Wang, Z.; Wang, Y.; Wang, Z.; Zhao, J.; Gutkind, J. S.; Srivatsan, A.; Zhang, G.; Liao, H. S.; Fu, X.; Jin, A.; Tong, X.; Niu, G.; Chen, X. *ACS Nano* **2015**, *9*, 6683.
(58) Subramanian, A.; Krishnan, U. M.; Sethuraman, S. J. *J. Biomed. Sci.* **2009**, *16*, 108.
(59) Colon-Ramos, D. A. *Curr. Top. Dev. Biol.* **2009**, *87*, 53.
(60) De Camilli, P.; Cameron, R.; Greengard, P. *J. Cell Biol.* **1983**, *96*, 1337.
(61) Carlson, A. L.; Bennett, N. K.; Francis, N. L.; Halikere, A.; Clarke, S.; Moore, J. C.; Hart, R. P.; Paradiso, K.; Wernig, M.; Kohn, J.; Pang, Z. P.; Moghe, P. V. *Nat. Commun.* **2016**, *7*, 10862.


DOI: 10.1021/jacs.6b09014
*J. Am. Chem. Soc.* 2016, 138, 15027−15034